An hp-adaptive quadrature method for irregular integrands: Application to the population balance equation birth term

Mathias Engh*, Jannike Solsvik, Hugo A. Jakobsen

Department of Chemical Engineering, Norwegian University of Science and Technology, N-7491 Trondheim, Norway

Abstract

The solution of the population balance equation requires the integration of several source terms. In the numerical weighted residuals methods, Gaussian quadrature is a natural candidate for numerical integration. Previous works using the weighted residuals methods for solving the population balance equation did use a fixed grid of quadrature points. This work shows that the use of adaptive quadrature points for the numerical integration can lead to more efficient and accurate solutions of the equation. For cases where the integrand shows a high degree of irregularity, the hp-optimization method distributes the quadrature points such that the method becomes more efficient than with a fixed grid. An additional improvement is that the amount of quadrature points changes to fit the need for each integral present, rather than having one set of quadrature points for all cases. A simple population balance model demonstrates the use of the adaptive quadrature approach.

Keywords: Population balance; Adaptive quadrature; hp-adaptive; Weighted residual methods; Bubble Column; Multiphase flow

1. Introduction

The modelling of dispersed systems is a relatively common occurrence in a variety of chemical engineering applications. Examples include modelling

*Corresponding author

Email addresses: mathias.engh@ntnu.no (Mathias Engh), jannike.solsvik@ntnu.no (Jannike Solsvik), hugo.a.jakobsen@ntnu.no (Hugo A. Jakobsen)

of crystallization processes, polymerization reactions and dispersed multiphase flows. An excellent tool for describing such dispersed systems is the population balance equation (PBE) (Ramkrishna, 2000). The PBE is an integro-differential equation which describes the evolution of a continuous density function. This density function describes the amount of the dispersed phase in all independent coordinates. Typical coordinates are time, external space and the inner coordinates. Usually only one inner coordinate is considered. The inner coordinate is often taken to be the diameter, volume or mass of the dispersed phase particles. The numerical solution of the PBE can often be a computationally demanding task. The books of Marchisio and Fox (2013) and Jakobsen (2014) present an excellent overview of typical numerical methods used to solve the PBE. The main methods presented in Marchisio and Fox (2013) are the class and sectional methods, the method of moments, the quadrature method of moments and the Monte Carlo methods. Of these methods, some of the advantages and disadvantages of the three first methods will be outlined.

In the class and sectional methods, the density function in the PBE is divided in several sections or classes. These sections are approximated using some discretisation techniques, often a zeroth or low order polynomial. The zeroth order polynomial representation represents the density function as a histogram. These types of methods require care when solving for the closure laws in order for the physical quantities to be conserved and correctly be transferred between the sections. An example of these types of methods is the Fixed Pivot technique of Kumar and Ramkrishna (1996). The finite volume method (FVM) can also be seen as belonging to the class and sectional methods. (Marchisio and Fox, 2013)

The popular method of moments (MOM) is based on solving a moment form of the PBE. The partial integro-differential equation is then rewritten as a set of ordinary differential equations by an averaging procedure. In this process the knowledge of the density function is lost. For some modelling purposes only the moments of the PBE are required. The moment methods are less compu-

tationally demanding and are thus often used for coupled CFD-PBE models (Jakobsen, 2014). In the recent years there has been an increasing interest in using the number or mass density function directly. When using the popular moment methods, reconstruction of the density function is required. Typically assumptions regarding the shape of the density function has to be made. Correct reconstruction of the continuous density function from the moment methods is a non-trivial task and is currently receiving attention in the population balance modelling field (Mead and Papanicolaou, 1984; Attarakih and Bart, 2018; Pigou et al., 2018).

The quadrature method of moments (QMOM), first proposed by Mcgraw (1997), is related to the method of moments. This method replaces the requirement of exact closure of the source terms with that of an approximate closure. The integral terms are approximated using Gaussian quadrature, and the density function is approximated as a sum of weighted Dirac delta functions. This allows the solution abscissas and weights to be varied rather than fixed. The advantage of this is that knowledge of only lower order moments of the density function is needed to solve the system. The problem is essentially changed from finding an exact solution for all the moments, to minimizing the error of the system by finding the best sets of solution abscissas and weights to satisfy the requirements of a few moments. This methods main challenge is that the procedure to calculate the optimum abscissas and weights can be rather complex. A problem associated with the original QMOM is related to the fact that the method stability limits the number of moments that might be applied thus limiting the accuracy of the method (Dorao, 2006). Other quadrature based method of moments (QBMM) have been proposed over the years, to overcome the problems associated with the original QMOM (Marchisio and Fox, 2005; Yuan and Fox, 2011; Nguyen et al., 2016). The Direct Quadrature Method of Moments (DQMOM), tracks the solution abscissas and weights directly, rather than the moment set of equations. The Extended Quadrature Method of Moments (EQMOM), is based on combining the QMOM with the

kernel density element method, through the addition of a parameter which adjusts the variance of the kernel densities according to an additional constraint (Yuan et al., 2012). Quadrature based moment methods have also been combined with sectional methods, giving rise to the sectional QMOM and sectional DQMOM (Attaraikh et al., 2009).

However, it is also possible to simply solve directly for the density function. Numerical methods such as spectral element and spectral methods can be used to obtain the density function. This direct approach comes with the major drawback of high computational costs. Some of the common commercial packages available for solving the PBE, such as PARSIVAL and PREDICI, do make use of the finite element Galerkin method (Wulkow et al., 2001; Yaghini and Iedema, 2014). More specifically this software has a self optimising grid that can vary both element size and polynomial order (hp-FEM) with the intention of reducing computational time and achieving satisfactory accuracy. Another option, residing under the spectral methods is the family of weighted residuals. These methods rely on approximating the exact solution through a set of basis polynomial functions which span the entire computational domain (Finlayson and Scriven, 1966). The fitting of these basis polynomials is dependent on the particular weighting functions used. Previous studies show that the orthogonal collocation method is perhaps the most suitable method from the weighted residual family for solving the PBE (Solsvik and Jakobsen, 2013a). Comparisons between the finite volume and the weighted residual methods for the solution of the PBE have shown that the FVM might be preferable (Solsvik et al., 2016). This is especially noticeable in cases where the density function contains steep gradients, due to the ease of implementing higher numerical resolution in the parts of the domain containing these gradients compared to spectral methods (Solsvik et al., 2016). These types of systems are not the typical domain of the spectral methods, and it is to expected that the FVM or FEM codes should perform better. There is another possible weakness of the weighted residual methods. The integral source terms containing irregular integrand functions

might not be resolved with sufficient accuracy. In particular the, the irregular behaviour of certain daughter size distribution function models might require further attention. The majority of these terms need to be integrated numerically.

A PBE with one inner coordinate describing a chemical engineering problem can take the following form:

$$\frac{\partial f(t,\mathbf{r},\xi)}{\partial t} + \mathbf{v}_{\mathbf{r}} \cdot \nabla_{\mathbf{r}} f(t,\mathbf{r},\xi) + v_{\xi} \frac{\partial f(t,\mathbf{r},\xi)}{\partial \xi} = S \tag{1}$$

where f is the density function and the independent coordinates are time, t, space, $\mathbf{r}$, and size, ξ. The source term accounts for the breakup or attrition, the aggregation or coalescence, the nucleation and dissolution of particles. Furthermore both the breakup and coalescence term can be separated into a positive and negative contribution:

$$\begin{aligned} S = -b_d(\xi) f(t,\mathbf{r},\xi) + \int_{\xi}^{\infty} b_b(t,\mathbf{r},\xi,\zeta) f(t,\mathbf{r},\zeta) \mathrm{d}\zeta \\ -f(t,\mathbf{r},\xi) \int_0^{\infty} c_d(t,\mathbf{r},\xi,\zeta) f(t,\mathbf{r},\zeta) \mathrm{d}\zeta + \int_0^{\xi} c_b(t,\mathbf{r},\xi,\zeta) f(t,\mathbf{r},\zeta) f(t,\mathbf{r},\xi-\zeta) \mathrm{d}\zeta \\ + J_{nuc}(t,\mathbf{r},\xi) - J_{dis}(t,\mathbf{r},\xi) f(t,\mathbf{r},\xi) \end{aligned} \tag{2}$$

where it can be seen that there are three integral source terms. $b_d(t,\mathbf{r},\xi)$, $b_b(t,\mathbf{r},\xi,\zeta), c_d(t,\mathbf{r},\xi,\zeta)$, $c_b(t,\mathbf{r},\xi,\xi-\zeta)$, $J_{nuc}(t,\mathbf{r},\xi)$ and $J_{dis}(t,\mathbf{r},\xi)$ represents the various closures needed. In most previous work the solution of the PBE using weighted residual methods, a fixed number of quadrature points has been used for the integration of these source terms, see e.g. the works of (Zhu et al., 2008; Nayak et al., 2011; Vik et al., 2018). In these works the number of quadrature points and collocation points are the same. For clarity, the distinction between quadrature points and collocation points is elucidated. Quadrature points are the points where the integrand is evaluated, whereas collocation points are the

point where the partial differential equation is evaluated in the weighted residual methods. In order to ensure an accurate solution, a large number of both quadrature and collocation points may be used.

For solving the PBE for highly coupled systems, neither under integration nor too few collocation points are desired. The use of too few collocation points means that the density function is not completely resolved. Under integration is a result of too few quadrature points and leads an inaccurate approximation of the integral source terms. A system of equations that is as big as necessary, but no bigger, would keep computational costs down. If it were possible to construct an efficient grid once for a specific PBE application and reuse the same grid throughout the computations this may lead to improved computational performance. During previous work in the research group, it has been experienced that some of the breakage closures used have tendency to be under integrated (Zhu et al., 2008; Nayak et al., 2011; Solsvik and Jakobsen, 2013a; Vik et al., 2018). A set of quadrature points which will efficiently approximate the integral source term would be welcome.

This paper proposes a novel method of reducing the number of quadrature points needed for an accurate solution of the PBE source terms using the orthogonal collocation method. The method takes into account the mathematical behaviour of the kernel functions, and distributes the quadrature points to achieve sufficiently accurate and efficient integration. It is noted that the emphasis is placed mainly on the regularity of the daughter size distribution function rather than the regularity of the density function. The implementation of an adaptive quadrature is aided by the use of a hp-optimization method. A simple population balance model has been used for demonstration of the method. The solution of the PBE with the adaptive grid points will be compared with respect to accuracy to that of the fixed quadrature solution with respect to the mass conserving properties of the system.

The article has the following outline: In section 2 the mathematical tools necessary will be presented, while section 3 gives the basics of the adaptive quadra-

ture formulation. Furthermore section 4 shows the implementation strategy for the standard orthogonal collocation solver, and the link between the adaptive quadrature and fixed quadrature solver is explained. The traditional approach of using the same number of collocation and quadrature points will be used for the fixed grid approach. The results and discussion is presented in section 5 before we arrive at our conclusion in section 6.

2. Basic Concepts of Weighted Residual Methods

The theory behind the weighted residual methods, as well as required background theory will be described in this section. For a thorough mathematical examination, the reader is referred to the works of Finlayson and Scriven (1966); Canuto et al. (2006); Quarteroni (2014); Karniadakis and Sherwin (2005), whose works are the basis of this section. Given a general problem on the form:

$$\mathcal{L}u(x) = g(x) \quad \text{in} \quad \Omega \tag{3}$$

$$\mathcal{B}u(x) = s(x) \quad \text{on} \quad \partial\Omega \tag{4}$$

where $\mathcal{L}$ and $\mathcal{B}$ are linear operators corresponding to the differential equation and boundary condition respectively. The computational domain is denoted by Ω and the boundary of the domain by $\partial\Omega$. The function to be approximated is $u(x)$ and the corresponding source terms are $g(x)$ and $s(x)$. The approximation of the unknown function is often based on a truncated series expansion taking the form:

$$u(x) \approx u_N(x) = \sum_{j=0}^{N} \alpha_j \phi_j^N(x) \tag{5}$$

where α_j are basis coefficients and $\phi_j^N(x)$ are basis polynomials of order N. An often used basis polynomial is the Lagrange polynomial defined as:

$$l_j^N(x) = \prod_{\substack{i=0 \\ j \neq i}}^{N} \frac{x - x_i}{x_j - x_i} \tag{6}$$

with the important property:

$$l_j^N(x_i) = \begin{cases} 1 & \text{if} \quad i = j \\ 0 & \text{if} \quad i \neq j \end{cases} \tag{7}$$

where the index i represents the collocation point and the index j denotes the basis polynomial. The use of a Lagrange basis polynomial means that the approximation takes a *nodal* form. This has the effect that the basis coefficient correspond to the function value at the given collocation point. The function approximation can thus be written as:

$$u(x) \approx u_N(x) = \sum_{j=0}^{N} u_j l_j^N(x) \tag{8}$$

where the unknowns are simply the basis coefficients, i.e. the discrete function values at the given collocation points. This type of approximation can also be used to interpolate between a set of points. Furthermore, the choice of Lagrange polynomials implies that the computational domain is finite. Introducing the residual definition:

$$\mathcal{R}(x; u_0, u_1, ..., u_N) = \mathcal{L}u_N(x) - g(x) = \sum_{j=0}^{N} u_j \mathcal{L} l_j^N(x) - g(x) = 0 \tag{9}$$

the next problem arising is how to select the basis coefficients which meet this criteria. The solution of the weighted residual methods is to take the inner product of this residual definition and a weighting function:

$$\int_\Omega \mathcal{R}(x; u_0, u_1, ..., u_N) w_i(x) \mathrm{d}x = 0, \quad \forall i \tag{10}$$

where the choice of weighting function defines the numerical method. If the Dirac delta function is chosen as the weighting function, the result is the orthogonal collocation method. The inclusion of the Dirac delta function as weight

means that the residual is to be minimized at the collocation points only, as the integral over $\delta(x - x_i)$ is unity if x_i is in the integration domain. The following result is achieved:

$$\sum_{j=0}^{N} u_j \mathcal{L} l_j^N(x_i) - g(x_i) = 0, \quad \forall i \tag{11}$$

which means that the solution is enforced only at the given collocation points. This leads to a straightforward connection between the differential equation and the algebraic equation system. For the approximation of the derivative, it is sufficient to take the derivative of the Lagrange interpolating polynomial. For a given collocation point x_i this can be done in the following way:

$$\frac{\partial u(x_i)}{\partial x} \approx \frac{\partial u^N(x_i)}{\partial x} = \sum_{j=0}^{N} u_j \frac{\partial l_j^N(x_i)}{\partial x} \tag{12}$$

The different evaluations of the Lagrange derivatives can be stored in a matrix, where the following notation is introduced for simplicity:

$$\mathbf{D}_{i,j} = \frac{\partial l_j^N(x_i)}{\partial x} \tag{13}$$

which makes it possible to find an approximation of the derivative at a given point in the following way:

$$\frac{\partial u^N(x_i)}{\partial x} = \mathbf{D}_{i,*}\mathbf{u} \tag{14}$$

where $\mathbf{u}$ is a vector containing the function values at the given node points corresponding to the basis polynomials, $\mathbf{u} = \Big(u_0, u_1, ..., u_N\Big)^T$. The collocation points are found by taking the roots of select Jacobi polynomials. The Lagrange basis polynomials through the Legendre root collocation points have a maximum absolute value of unity. This leads to the lowest growth of the Lebesgue constant. The Lebesgue constant is related to the interpolation error of the polynomials, with a smaller constant leading to a smaller maximum error. The Gauss-Lobatto-Legendre (GLL) points can furthermore be extended to have the

lowest interpolation error also in two-dimensional quadrilateral domains (Karniadakis and Sherwin, 2005). The Golub-Welsch algorithm is frequently used to find the Legendre polynomial roots (Golub and Welsch, 1969). Faster algorithms have been presented in recent times, such as the method of Hale and Townsend (2013).

The Legendre polynomial has more uses than being the source of the GLL collocation points. In Gaussian quadrature, the numerical integration of a function $u(x)$ is given as:

$$\int_{-1}^{1} u(x)\mathrm{d}x \approx \sum_{i_q=0}^{N_q} w_{i_q}(-1,1)u(x_{i_q}) \tag{15}$$

where the continuous function $u(x)$ is being evaluated at a set of N_q points, known as quadrature points. It is stressed that N_q is not necessarily the same as N. These quadrature points are found in the same way as the GLL collocation points. The weight, w_{i_q}, depends on the location of the points and the order of the approximation. Using a Gauss-Lobatto quadrature, the integration is exact if $u(x) \in \mathcal{Q}_{2N_q-1}$, where $\mathcal{Q}_{2N_q-1}$ is the polynomial space containing polynomials up to order $2N_q - 1$. The quadrature weights are found in the following way (Quarteroni, 2014):

$$w_{i_q}(-1,1) = \frac{2}{N_q(N_q+1)} \frac{1}{[L_{N_q}(x_{i_q})]^2}, \quad i_q = 0, ..., N_q \tag{16}$$

where i_q is an index describing the quadrature point. In order to find the Legendre polynomials the following recursive relationship can be used (Quarteroni, 2014)

$$L_{k+1}(x) = \frac{2k+1}{k+1} x L_k(x) - \frac{k}{k+1} L_{k-1}(x) \tag{17}$$

with $L_0 = 1$ and $L_1 = x$. With the use of GLL points, there also exists the following analytic relationship between the Lagrange and the Legendre polynomials:

$$l_j^N(x) = \frac{-1}{N(N+1)} \frac{(1-x^2)L'_N(x)}{(x-x_j)L_N(x_j)} \tag{18}$$

where the prime notation means the derivative with respect to x. Furthermore it is possible to use the Legendre polynomial as a basis in the truncated series expansion presented in (5):

$$u(x) \approx \hat{u}_N(x) = \sum_{k=0}^{N} \hat{a}_k L_k(x) \tag{19}$$

where $\hat{a}_k$ is the basis coefficient and L_k is the kth order Legendre polynomial. Furthermore $\hat{u}_N(x)$ converges to $u(x)$ in the $\mathrm{L}^2(-1,1)$ norm. This is gives rise to a *modal* type of approximation. In this approximation the change of a basis coefficient changes the solution at all other node points. Increasing the polynomial order to infinity leads to the following sequence (Quarteroni, 2014):

$$\lim_{N\to\infty} \|u - \hat{u}_N\|^2_{\mathrm{L}^2(-1,1)} = 0 \tag{20}$$

which is equivalent to:

$$\lim_{N\to\infty} \| \sum_{k=N+1}^{\infty} \hat{a}_k L_k\|_{\mathrm{L}^2(-1,1)} = 0 \tag{21}$$

by applying Parseval's identity, the $\mathrm{L}^2(-1,1)$ norm can be expressed as:

$$\|u - \hat{u}_N\|^2_{\mathrm{L}^2(-1,1)} = \sum_{k=N+1}^{\infty} \frac{\hat{a}_k^2}{k+\frac{1}{2}} \tag{22}$$

which gives the error of the best polynomial approximation in the L^2-norm, also known as the truncation error (Canuto et al., 2006). Furthermore, if $u \in \mathrm{H}^s(-1,1)$ with $s \geq 0$, then there exists a constant $C_s > 0$ to satisfy:

$$\|u - \hat{u}_N\|_{\mathrm{L}^2(-1,1)} \leq C_s \left(\frac{1}{N}\right)^s \|u^{(s)}\|_{\mathrm{L}^2(-1,1)} \tag{23}$$

which is to say that the convergence rate of the numerical approximation is higher the more regular the exact solution is (Quarteroni, 2014). The space $H^s(\Omega)$ is defined as:

$$H^s(\Omega) = \{u \in L^2(\Omega) : D^\alpha u \in L^2(\Omega) \quad \forall \alpha : |\alpha| \leq s\} \tag{24}$$

where the distributional derivative has been used. The use of the Gaussian quadrature is a natural choice for the weighted residual methods. The numerical integration exactly integrates the interpolating function (Quarteroni, 2014). The upper bounded error in the L_2-norm of the interpolating operator (18) is given as:

$$\|u - \mathrm{I}_\mathrm{N}^\mathrm{GLL} u\|_{\mathrm{L}^2(-1,1)} \leq C_s \left(\frac{1}{N}\right)^s \|u^{(s)}\|_{\mathrm{L}^2(-1,1)} \tag{25}$$

where I_N^{GLL} has been used as notation for the Nth order interpolating polynomial through a set of GLL points. As the integration rules are based on the interpolating polynomials, there also exist a relationship similar to (25) for the error bounds of the integration (Quarteroni, 2014):

$$\left| \int_{-1}^{1} u(x)\mathrm{d}x - \sum_{i_q=0}^{N_q} w_{i_q}(-1,1)u(x_{i_q}) \right| \leq C_s \left(\frac{1}{N}\right)^s \|u^{(s)}\|_{\mathrm{L}^2(-1,1)} \tag{26}$$

where an important detail is that the order of convergence is higher the more regular a function is. It should be noted that the constants C_s are not necessarily the same in (23), (25) and (26). The errors do however decrease asymptotically at the same rate (Canuto et al., 2006). If certain parts of the integration domain are more regular than other parts, it might be beneficial to divide the integral into several parts with a different amount of quadrature points for each integral depending on the regularity of the integrated function.

3. Adaptive Quadrature

The rate of convergence for the integral calculation depends on the regularity of the integrand. The regularity is in this case related to the differentiability of the integrand. The goal of the adaptive quadrature is to find the most efficient way of calculating the integral. An option for solving the integral efficiently is to separate the integration domain into several smaller ones and to use an appropriate quadrature order for each of these integration domains. These domains will be referred to as elements. An integral can thus be written in the following way using elements:

$$\int_{\Omega} u(x)\mathrm{d}x = \sum_{e=1}^{E} \int_{\Omega_e} u(x)\mathrm{d}x \approx \sum_{e=1}^{E} \sum_{i_q=0}^{N_q,e} w_{i_q,e}(x_{0,e}, x_{N_q,e}) u(x_{i_q,e}) \qquad (27)$$

where the there are E elements, indexed by e. By examining the regularity of the integral kernel, it is possible to estimate if the integration error decreases more by using a higher amount of quadrature points in one of the integration elements, or by adding more elements. The regularity is found by using the root test algorithm of Houston and Süli (2005) and Houston et al. (2003). The method is based on examining the decay rate of the basis coefficient, a_k, for the Legendre approximation of the function, (19). The available numerically estimated expansion coefficient of highest order is compared to the polynomial order to determine the regularity. The set of numerical Legendre coefficients, a_k, can be found by solving the matrix system $\mathbf{Va} = \mathbf{u}$ where $\mathbf{V}$ is a matrix of the Legendre polynomial values at the set of quadrature points, $L_k(x_{i_q})$, $\mathbf{a}$ is a vector of basis coefficients, a_k, and $\mathbf{u}$ is a vector of function values at the quadrature points, $u(x_{i_q})$ (Canuto et al., 2006). $\mathbf{V}$ is known as the generalized Vandermonde matrix. The three matrices are given as:

$$\mathbf{V} = \begin{pmatrix} L_0(x_0) & L_1(x_0) & \cdots & L_N(x_0) \\ L_0(x_1) & L_1(x_1) & \cdots & L_N(x_1) \\ \vdots & \vdots & \ddots & \vdots \\ L_0(x_N) & L_1(x_N) & \cdots & L_N(x_N) \end{pmatrix} \tag{28}$$

$$\mathbf{a} = \begin{pmatrix} a_0 \\ a_1 \\ \vdots \\ a_N \end{pmatrix} \tag{29}$$

$$\mathbf{u} = \begin{pmatrix} u(x_0) \\ u(x_1) \\ \vdots \\ u(x_N) \end{pmatrix} \tag{30}$$

Alternatively the coefficients can be found by the following relation:

$$\hat{a}_k = \frac{2k+1}{2} \int_{-1}^{1} u(x) L_k(x) \mathrm{d}x \tag{31}$$

It should be noted that in order to find the *exact* coefficients numerically, an infinite amount of points would have to be used. In the matrix inversion procedure, a numerical approximation of the modal basis coefficients is found, a_k. The regularity estimator is given as:

$$\sigma = \frac{\log(2N+1) - \log(2|a_N|^2)}{2\log N} - \frac{1}{2} \tag{32}$$

where the available basis coefficient of highest order is used, a_N. The function is classified as sufficiently regular if the following criteria is fulfilled:

$$\sigma > N + 1 \tag{33}$$

this criteria has previously been used to find the regularity of the density function for the PBE (Dorao and Jakobsen, 2008), but it can equally well be used to find the regularity of the kernels for the source terms.

The relationship between the interpolation and integration error can be used in order to approximate the accuracy of the integral. We propose an heuristic procedure in order to know if the integral is approximated sufficiently. It is based on the same Legendre basis coefficients found through the Vandermonde matrix. Using a truncated form of (22) we get an approximation of the interpolation accuracy:

$$\|u - \mathbf{I}_N^{GLL} u\|^2_{\mathrm{L}^2(-1,1)} \approx \|u - \hat{u}_N\|^2_{\mathrm{L}^2(-1,1)} \approx \sum_{k=N+1}^{P} \frac{a_k^2}{k + \frac{1}{2}} \tag{34}$$

Where we have neglected the potential influence of aliasing errors. As the interpolation and integration errors are proportional with a factor $(2N-1)/2$, it is possible to estimate the quadrature order necessary as $N/2+1$ relative to the order needed for sufficient interpolation.

4. Case study and implementation

In order to asses the numerical performance of the adaptive quadrature approach a case study is needed. In this work a steady state bubble column model is used. The diameter based mass density population balance equation for breakage dominated bubbly flows through a column can be written as (Solsvik and Jakobsen, 2013b):

$$\begin{aligned} v_z \frac{\partial f_{d,m}(z,\xi)}{\partial z} - \frac{\xi v_z}{3\rho_d(z)} \frac{\partial \rho_d(z)}{\partial z} \frac{\partial f_{d,m}(z,\xi)}{\partial \xi} - f_{d,m}(z,\xi) \frac{v_z}{3\rho_d(z)} \frac{\partial \rho_d(z)}{\partial z} = \\ - b(\xi) f_{d,m}(z,\xi) + V(\xi) \int_{\xi}^{\xi_{max}} h(\xi,\zeta) b(\zeta) \frac{f_{d,m}(z,\zeta)}{V(\zeta)} \mathrm{d}\zeta \end{aligned} \tag{35}$$

where $f_{d,m}(z,\xi)$ is the diameter based mass density, v_z is the velocity through the reactor which is assumed constant, $\rho_d(z)$ is the density of the dispersed phase computed from the ideal gas law, $V(\xi)$ is the volume of the bubbles, $h(\xi,\zeta)$ is the daughter size redistribution function and $b(\xi)$ is the breakage frequency. The bubbles are in this case assumed to be perfectly spherical. The two independent

coordinates are the reactor axis, z, and the bubble diameter, ξ. Note that a finite range of sizes ranging from ξ_{min} to ξ_{max} has been considered for the bubble diameter. This gives a computational domain of $\Omega = [z_0, z_{\text{end}}] \times [\xi_{min}, \xi_{max}]$. The PBE (35) is a linear equation in $f_{d,m}$ as the coalescence terms have been neglected. The terms on the left hand side denote the changes in the distribution function due to advection in the axial direction, and the growth of bubbles related to change in gas phase density. To compute the dispersed phase density (gas density from ideal gas law) we assume isothermal conditions and the pressure gradient is assumed to be due to the weight of the liquid column solely, neglecting the gas phase fraction. The terms on the right hand side represent the death and birth processes of bubbles due to breakage. Binary breakage has been assumed. In order to solve this problem, an appropriate set of closures are required for the source terms. The first set of closures used in this work is taken from Coulaloglou and Tavlarides (1977):

$$b(\xi) = \frac{k_1 \epsilon^{1/3}}{\xi^{2/3}} \exp\left(-\frac{\sigma k_2}{\rho_l \epsilon^{2/3} \xi^{5/3}}\right) \tag{36}$$

$$h(\xi, \zeta) = \frac{72}{5} \frac{\xi^2}{\zeta^3} \exp\left(-\frac{9}{2} \frac{[2\xi^3 - \zeta^3]^2}{\zeta^6}\right) \tag{37}$$

where k_1 and k_2 are adjustable parameters, ϵ is the turbulent energy dissipation rate, σ is the surface tension and ρ_l is the liquid phase density. The approach of Prince and Blanch (1990) for gas-liquid flows is followed, meaning that the continuous phase density has been used rather than the dispersed phase density in (36). Another set of closures is used for further model validation is a version of the Martinez-Bazan et al. (2010) breakage kernel with a modified breakage probability as presented in Solsvik et al. (2017):

$$b(\xi) = \begin{cases} 0 & \text{if} \quad \xi < \xi_{\text{crit}} \\ \exp\left(\frac{-c_1 \sigma (\xi - \xi_{\text{crit}})^2}{\rho_d (\xi - \xi_{\text{crit}})^3 \epsilon^{2/3} \xi^{2/3}}\right) \frac{\sqrt{\beta [\epsilon \xi]^{2/3} - \frac{12\sigma}{\rho_l \xi}}}{\xi} & \text{if} \quad \xi > \xi_{\text{crit}} \end{cases} \tag{38}$$

$$h(\xi,\zeta) = \frac{1}{\zeta}\frac{\omega^2\left[\omega^{2/3}-\frac{1}{We_t}\right]\left[(1-\omega^3)^{2/9}-\frac{1}{We_t}\right]}{\int_{\omega_{min}}^{\omega_{max}}\left[\eta^{2/3}-\frac{1}{We_t}\right]\left[(1-\eta^3)^{2/9}-\frac{1}{We_t}\right]\mathrm{d}\eta} \tag{39}$$

$$\xi_{\text{crit}} = \left[\frac{12\sigma}{\rho_l\beta}\right]^{3/5}\epsilon^{-2/5} \tag{40}$$

$$\omega_{\min} = \left[\frac{\xi_{\text{crit}}}{\zeta}\right]^{\frac{5}{2}} \tag{41}$$

$$\omega_{\max} = (1-\omega_{\min}^3)^{1/3} \tag{42}$$

$$We_t = \frac{\xi^{5/3}}{\epsilon^{2/3}}\frac{\rho_l\beta}{12\sigma} \tag{43}$$

where it can be seen that breakage only occurs if the bubble has a diameter larger than ξ_{crit}. c_1 is a system parameter, β is a turbulence parameter and ω is the dimensionless daughter diameter, given as $\omega = \xi/\zeta$. In addition there is a minimum size of the bubble that can be created from breakage. This minimum size is given as a function of the critical bubble diameter and the mother diameter. The daughter redistribution function is normalized. The hydrostatic pressure, gas phase density and the change in density are found as:

$$p(z) = p_0 + \rho_l g(z_{end} - z) \tag{44}$$

$$\rho_d(z) = \frac{p(z)\bar{M}_m}{RT} \tag{45}$$

$$\frac{\partial\rho_d}{\partial z} = -\frac{\rho_d(z)}{p(z)}\rho_l g = -\frac{\bar{M}_m}{RT}\rho_l g \tag{46}$$

where $\bar{M}_m$ is the average molar mass of the dispersed phase, g is the gravitational acceleration, R is the universal gas constant, p is the pressure and T is the temperature. There are two initial conditions necessary to solve this model. At the inlet to the column a Dirichlet condition is imposed:

$$f_{d,m}(z_0,\xi) = 29.4\left[\frac{(b-a)\xi}{\xi_{max}-\xi_{min}}\right]^3 \exp\left(-0.7\left[\frac{(b-a)\xi}{\xi_{max}-\xi_{min}}\right]^4\right) \tag{47}$$

where $a = 10^{-3}$ and $b = 3$. Furthermore, the inlet condition in the ξ direction is given as:

$$f_{d,m}(z,\xi_{min}) = 29.4\left[\frac{(b-a)\xi_{min}}{\xi_{max}-\xi_{min}}\right]^3 \exp\left(-0.7\left[\frac{(b-a)\xi_{min}}{\xi_{max}-\xi_{min}}\right]^4\right) \tag{48}$$

4.1. Numerical implementation

A general implementation for solving the model equation with the orthogonal collocation method using standard fixed grid Gaussian quadrature will be presented. Using the orthogonal collocation method, without numerically approximating the integral, (35) can be approximated as:

$$\begin{aligned} v_z \sum_{j_z=0}^{N_z}\sum_{j_\xi=0}^{N_\xi} \frac{\partial l_{j_z}^{N_z}(z_{i_z})}{\partial z} l_{j_\xi}^{N_\xi}(\xi_{i_\xi}) f_{j_z,j_\xi} + \frac{\xi_{i_\xi} v_z \rho_l g}{3p(z_{i_z})} \sum_{j_z=0}^{N_z}\sum_{j_\xi=0}^{N_\xi} l_{j_z}^{N_z}(z_{i_z}) \frac{\partial l_{j_\xi}^{N_\xi}(\xi_{i_\xi})}{\partial \xi} f_{j_z,j_\xi} \\ + \frac{v_z \rho_l g}{3p(z_{i_z})} \sum_{j_z=0}^{N_z}\sum_{j_\xi=0}^{N_\xi} l_{j_z}^{N_z}(z_{i_z}) l_{j_\xi}^{N_\xi}(\xi_{i_\xi}) f_{j_z,j_\xi} + b(\xi_{i_\xi}) \sum_{j_z=0}^{N_z}\sum_{j_\xi=0}^{N_\xi} l_{j_z}^{N_z}(z_{i_z}) l_{j_\xi}^{N_\xi}(\xi_{i_\xi}) f_{j_z,j_\xi} \\ - V(\xi_{i_\xi}) \sum_{j_z=0}^{N_z}\sum_{j_\xi=0}^{N_\xi} \int_{\xi_{i_\xi}}^{\xi_{max}} l_{j_z}^{N_z}(z_{i_z}) l_{j_\xi}^{N_\xi}(\zeta) h(\xi_{i_\xi},\zeta) b(\zeta) \frac{f_{j_z,j_\xi}}{V(\zeta)} \mathrm{d}\zeta = 0 \end{aligned} \tag{49}$$

where the index j_ξ and j_z describe the basis polynomial for the ξ and z direction respectively. The indexes i_ξ and i_z describe which collocation point the basis polynomial is evaluated. N_ξ and N_z is the polynomial order of the numerical approximation in each dimension. The basis coefficients are indexed as f_{j_z,j_ξ}, as the collocation points are used for both dimensions. Notice how the integration variable in (49), ζ, is still a continuous variable. Implementing standard Gaussian quadrature rules, (35) can be approximated as:

$$v_z \sum_{j_z=0}^{N_z} \sum_{j_\xi=0}^{N_\xi} \frac{\partial l_{j_z}^{N_z}(z_{i_z})}{\partial z} l_{j_\xi}^{N_\xi}(\xi_{i_\xi}) f_{j_z,j_\xi} + \frac{\xi_{i_\xi} v_z \rho_l g}{3p(z_{i_z})} \sum_{j_z=0}^{N_z} \sum_{j_\xi=0}^{N_\xi} l_{j_z}^{N_z}(z_{i_z}) \frac{\partial l_{j_\xi}^{N_\xi}(\xi_{i_\xi})}{\partial \xi} f_{j_z,j_\xi}$$
$$+ \frac{v_z \rho_l g}{3p(z_{i_z})} \sum_{j_z=0}^{N_z} \sum_{j_\xi=0}^{N_\xi} l_{j_z}^{N_z}(z_{i_z}) l_{j_\xi}^{N_\xi}(\xi_{i_\xi}) f_{j_z,j_\xi} + b(\xi_{i_\xi}) \sum_{j_z=0}^{N_z} \sum_{j_\xi=0}^{N_\xi} l_{j_z}^{N_z}(z_{i_z}) l_{j_\xi}^{N_\xi}(\xi_{i_\xi}) f_{j_z,j_\xi}$$
$$- V(\xi_{i_\xi}) \sum_{j_z=0}^{N_z} \sum_{j_\xi=0}^{N_\xi} \sum_{i_q=0}^{N_q} l_{j_z}^{N_z}(z_{i_z}) l_{j_\xi}^{N_\xi}(\zeta_{i_q}) h(\xi_{i_\xi}, \zeta_{i_q}) b(\zeta_{i_q}) \frac{f_{j_z,j_\xi}}{V(\zeta_{i_q})} w_{i_q}(\xi_{i_\xi}, \xi_{max}) = 0 \tag{50}$$

the order of the quadrature approximation is given by N_q, and the quadrature index is given as i_q. The quadrature points and weights have been mapped from the standard domain in order to correspond to the computational domain between ξ_{i_ξ} and ξ_{max}. The geometry map from (-1,1) to (ξ_{i_ξ}, ξ_{max}) is given by:

$$\zeta_{i_q}(\xi_{i_\xi}, \xi_{max}) = \zeta_{i_\zeta}(-1,1)\frac{\xi_{max} - \xi_{i_\xi}}{2} + \frac{\xi_{max} + \xi_{i_\xi}}{2} \tag{51}$$

$$w_{i_q}(\xi_{i_\xi}, \xi_{max}) = w_{i_q}(-1,1)\frac{\xi_{max} - \xi_{i_\xi}}{2} \tag{52}$$

which means that a standard set of quadrature points can be easily mapped to the corresponding computational domain using (52). Figure 1 shows the relationship between the quadrature points, ζ_{i_q}, and the collocation points, ξ_{i_ξ}. The Lagrange basis polynomial evaluated at the quadrature points is computed from (18), making it possible to relate the function values at the quadrature and collocation points. This is done using (8):

$$f(\zeta_{i_q}) = \sum_{j_\xi=0}^{N_\xi} f_{j_\xi} l_{j_\xi}^{N_\xi}(\zeta_{i_q}) \tag{53}$$

As can be seen in (50), the only unknowns in the equation are the basis coefficients, f_{j_z,j_ξ}. The system of algebraic equations may be arranged on the form $\mathbf{Ax} = \mathbf{b}$, where $\mathbf{x}$ in this case is a vector of basis coefficients, f_{j_z,j_ξ}, corresponding to each collocation point. In the case that the PBE contains breakage

only, $\mathbf{b} = \mathbf{0}$. The matrix $\mathbf{A}$ can be indexed by I and J, $\mathbf{A}_{I,J}$, corresponding to the global collocation point index and the global basis polynomial index respectively. The relationships between the global index and the local indices are given by:

$$I = i_z(N_\xi + 1) + i_\xi \tag{54}$$

$$J = j_z(N_\xi + 1) + j_\xi \tag{55}$$

which means that it is possible to construct each entry in the matrix $\mathbf{A}$ by using (50) denoting the global index for each collocation point and basis polynomial. The global amount of collocation points is given by:

$$N_G = (N_z + 1)(N_\xi + 1) \tag{56}$$

and the basis coefficients and the product of the two sets of Lagrange polynomial are conveniently given as:

$$f_J = f_{j_z} f_{j_\xi} \tag{57}$$

$$l_J^{N_G}(z, \xi) = l_{j_z}^{N_z}(z) l_{j_\xi}^{N_\xi}(\xi) \tag{58}$$

which makes it possible to write (50) as:

$$\begin{aligned} v_z \sum_{J=0}^{N_G} \frac{\partial l_J^{N_G}(z_I, \xi_I)}{\partial z} f_J + \frac{\xi_I v_z \rho_l g}{3p(z_I)} \sum_{J=0}^{N_G} \frac{\partial l_J^{N_G}(z_I, \xi_I)}{\partial \xi} f_J \\ + \frac{v_z \rho_l g}{3p(z_I)} \sum_{J=0}^{N_G} l_J^{N_G}(z_I, \xi_I) f_J + b(\xi_I) \sum_{J=0}^{N_G} l_J^{N_G}(z_I, \xi_I) f_J \\ - V(z_I, \xi_I) \sum_{J=0}^{N_G} f_J \sum_{i_q=0}^{N_q} l_J^{N_G}(z_I, \zeta_{i_q}) h(\xi_I, \zeta_{i_q}) b(\zeta_{i_q}) \frac{1}{V(\zeta_{i_q})} w_{i_q}(\xi_I, \xi_{max}) = 0 \end{aligned} \tag{59}$$

with the assembling to the system matrix for the orthogonal collocation method taking the following form:

$$\mathbf{A}_{I,J} = v_z \frac{\partial l_J^{N_G}(z_I,\xi_I)}{\partial z} + \frac{\xi_I v_z \rho_l g}{3p(z_I)} \frac{\partial l_J^{N_G}(z_I,\xi_I)}{\partial \xi} + \frac{v_z \rho_l g}{3p(z_I)} l_J^{N_G}(z_I,\xi_I)$$
$$-b(\xi_I) l_J^{N_G}(z_I,\xi_I) + V(\xi_I) \sum_{i_q=0}^{N_q} l_J^{N_G}(z_I,\zeta_{i_q}) h(\xi_I,\zeta_{i_q}) b(\zeta_{i_q}) \frac{w_{i_q}(\xi_I,\xi_{max})}{V(\zeta_{i_q})} \tag{60}$$

where it can be seen that the use of a different index is still necessary for the quadrature points. The use of matrices for the interpolating polynomials leads to a significantly simplified implementation. The local index Lagrange polynomials can for instance be represented by an identity matrix for each independent coordinate:

$$l_{j_z}^{N_z}(z_{i_z}) = \mathbf{I}_{i_z,j_z} \tag{61}$$

A gathering matrix (GM) can be used in order to relate the local and the global indexes. The GM takes the local indexes as input and return the global index, defined by (54):

$$\mathrm{GM}_{i_z,i_\xi} = I \tag{62}$$

The GM will usually have a structure which is similar to that of Figure 2, where the entries of the matrix follows (54). A third type of matrix is also of help for interpolating from the collocation to the quadrature points. As opposed to the Lagrange polynomials evaluated at the collocation points, this is a full matrix:

$$l_{j_\xi}^{N_\xi}(\zeta_{i_q}) = \mathbf{Q}_{i_q,j_\xi}^{i_\xi} \tag{63}$$

it should be noted that this interpolating matrix only has a square structure if the amount of collocation and quadrature points is equal. This matrix has the following entries:

$$\mathbf{Q}^0 = \begin{pmatrix} l_0^{N_\xi}(\zeta_0) & l_1^{N_\xi}(\zeta_0) & \cdots & l_{N_\xi}^{N_\xi}(\zeta_0) \\ l_0^{N_\xi}(\zeta_1) & l_1^{N_\xi}(\zeta_1) & \cdots & l_{N_\xi}^{N_\xi}(\zeta_1) \\ \vdots & \vdots & \ddots & \vdots \\ l_0^{N_\xi}(\zeta_{N_q}) & l_1^{N_\xi}(\zeta_{N_q}) & \cdots & l_{N_\xi}^{N_\xi}(\zeta_{N_q}) \end{pmatrix} \tag{64}$$

As the set of quadrature points depends on the lower bound of the integration (the daughter size), the superscript i_ξ denotes which of the interpolating matrices is used. The span of the quadrature points are given as:

$$\zeta \in [\xi_{i_\xi}, \xi_{max}] \tag{65}$$

which means that a given index of ζ refers to a different location in property space depending on i_ξ, see Figure 1. Due to the use of GLL collocation points, the numerical value of the entries in $\mathbf{Q}$ range between -1 and 1. Interpolation from the collocation points to the quadrature points can be done by simple matrix operations:

$$\mathbf{f}_\zeta^{\xi_{i_\xi}} = \begin{pmatrix} f_{\zeta_0} \\ f_{\zeta_1} \\ \vdots \\ f_{\zeta_{N_q}} \end{pmatrix} = \mathbf{Q}^{i_\xi}\mathbf{f} \tag{66}$$

For a simple implementation of the orthogonal collocation method, multiple for-loops can be used. Among other alternatives is the use of the Kronecker product. An example of a simple implementation of the PBE model is given in pseudocode 1.

Pseudocode 1.

```
for j_z ← 0 to N_z do
    for j_ξ ← 0 to N_ξ do
        compute GM_{j_z,j_ξ} = J
        for i_z ← 0 to N_z do
            for i_ξ ← 0 to N_ξ do
                compute GM_{i_z,i_ξ} = I
                compute p(z_{i_z}); (44)
                compute ρ_d(z_{i_z}); (45)
                compute b(ξ_{i_ξ}); (36) or (38)
```

for $i_\xi \leftarrow 0$ **to** N_ξ **do**

for $j_z \leftarrow 0$ **to** N_z **do**

for $j_\xi \leftarrow 0$ **to** N_ξ **do**

$\mathbf{A}_{I,J} = v_z \mathbf{D}_{i_z,j_z} \mathbf{I}_{i_\xi,j_\xi} + \frac{\xi_{i_\xi} v_z \rho_l g}{3p(z_{i_z})} \mathbf{D}_{i_\xi,j_\xi} \mathbf{I}_{i_z,j_z} + \frac{v_z \rho_l g}{3p(z_{i_z})} \mathbf{I}_{i_z,j_z} \mathbf{I}_{i_\xi,j_\xi} - b(\xi_{i_\xi}) \mathbf{I}_{i_z,j_z} \mathbf{I}_{i_\xi,j_\xi}$

for $i_q \leftarrow 0$ **to** N_q **do**

compute $b(\zeta_{i_q})$; (36) or (38)

compute $h(\zeta_{i_q}, \xi_{i_\xi})$; (37) or (39)

$\mathbf{A}_{I,J} = \mathbf{A}_{I,J} + \frac{\xi_{i_\xi}^3}{\zeta_{i_q}^3} \mathbf{Q}_{i_q,j_\xi}^{i_\xi} h(\zeta_{i_q} \xi_{i_\xi}) b(\zeta_{i_q}) w_{i_q}(\xi_{i_\xi}, \xi_{max})$

end for

end for

end for

end for

end for

The initial conditions are imposed in a strong form consistent with the orthogonal collocation method. The Dirichlet conditions means that the basis coefficients for each of the corresponding collocation points is set to the prescribed value directly. The corresponding row in the system matrix $\mathbf{A}$ is set to zero for all entries except for the diagonal entry which is set to 1. The row in the source term $\mathbf{b}$ is calculated according to (47) or (48) depending on which condition is imposed. The first N_ξ rows of the system matrix take the following form:

$$\mathbf{A} = \begin{pmatrix} \begin{pmatrix} 1 & 0 & \cdots & 0 \\ 0 & \ddots & \cdots & 0 \\ \vdots & \vdots & \ddots & 0 \\ 0 & 0 & 0 & 1 \end{pmatrix} & \begin{pmatrix} 0 & 0 & \cdots & 0 \\ 0 & \ddots & \cdots & 0 \\ \vdots & \vdots & \ddots & 0 \\ 0 & 0 & 0 & 0 \end{pmatrix} & \begin{pmatrix} 0 & 0 & \cdots & 0 \\ 0 & \ddots & \cdots & 0 \\ \vdots & \vdots & \ddots & 0 \\ 0 & 0 & 0 & 0 \end{pmatrix} \end{pmatrix} \tag{67}$$

After assembling the system matrix and source term, the mass density distribution can be found at all the collocation points by solving the system of equations:

$$\mathbf{A}\mathbf{x} = \mathbf{b} \tag{68}$$

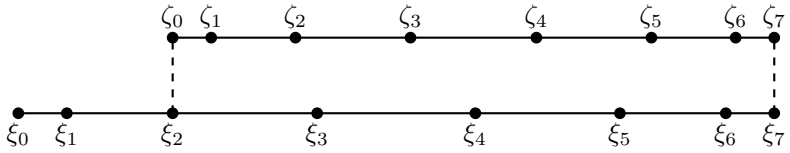

Figure 1: The relationship between the collocation points, ξ_{i_ξ}, for the mass density distribution and the quadrature points corresponding to different mother bubble sizes, ζ_{i_q}, in the breakage birth term. Note that both sets of points are distributed as GLL points.

It can be convenient to separate the five different terms of the PBE into five different operators. The total system matrix can be decomposed as follows:

$$\mathbf{A} = \mathbf{A}^{\text{Advection}} + \mathbf{A}^{\text{Growth}_1} + \mathbf{A}^{\text{Growth}_2} - \mathbf{A}^{\text{Birth}} + \mathbf{A}^{\text{Death}} \tag{69}$$

In this way it is possible to see the effect of each term simply by multiplying the operator with the calculated mass density distribution at the collocation points:

$$\text{Change due to bubble birth from breakage} = \mathbf{A}^{\text{Birth}}\mathbf{f}$$

In order to conserve mass in the bubble breakup process, the integral of the breakage death and birth contributions over the whole computational domain should be equal:

$$\int_\Omega \mathbf{A}^{\text{Birth}}\mathbf{f}\mathrm{d}\Omega = \int_\Omega \mathbf{A}^{\text{Death}}\mathbf{f}\mathrm{d}\Omega \tag{70}$$

which should also be true for each axial point in the reactor. This is because the bubbles lost due to breakage will reappear at the same point in physical space. In addition the mass flowing in and out of the tank should be equal. As the velocity is constant:

$$\int_{\Omega_\xi} \mathbf{f}^{\text{Inlet}}\mathrm{d}\xi = \int_{\Omega_\xi} \mathbf{f}^{\text{Outlet}}\mathrm{d}\xi \tag{71}$$

4.2. Solution with the standard method

Most of the following physical data and adjustable parameters for the model system has been taken from the work of Solsvik and Jakobsen (2013a). The

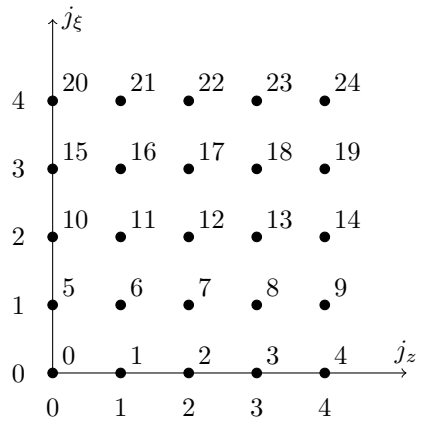

Figure 2: The relationship between the local indexes, j_z and j_ξ, and the global index J for two sets of GLL collocation points.

data is presented in Table 1.

Figures 3 and 4 shows the solution of PBE at the inlet, middle and outlet of the column using the Coulaloglou & Tavlarides and modified Martinez-Bazan breakage kernels respectively. Figures 5 and 6 show the behavior for the breakage frequency given by (36) for Coulaloglou & Tavlarides and (38) for the modified Martinez-Bazan. Figures 7 and 8 show the redistribution function using (37) for Coulaloglou & Tavlarides and (39) for the modified Martinez-Bazan. The chosen redistribution functions are shown to have a significant change in magnitude over a small difference in mother diameter. This effect is particularly large for smaller mother sizes. As can be seen from Figures 9 and 10 showing the integral kernels without the mass density function, and Figures 11 and 12 showing the integration kernel with the inlet mass density function. The effect of the redistribution function is retained and represented by the whole integrand function. When computing the breakage source integral, the large range of scales of the integrand require a relatively high order quadrature approximation for accurate numerical integration.

Parameter	Unit	Value
ξ_{min}	m	4×10^{-4}
ξ_{max}	m	2.62×10^{-2}
z_0	m	0
z_{end}	m	3
v_z	m s^{-1}	0.5
σ	N m^{-1}	0.072
ρ_l	kg m^{-3}	998
$\rho_{0,d}$	kg m^{-3}	1.188
p_0	Pa	101500
ϵ	m^2 s^{-2}	0.392
k_1	-	0.01
k_2	-	0.106
g	m s^{-2}	9.8
$\bar{M}_m$	kg mol^{-1}	0.029
R	J K^{-1} mol^{-1}	8.3145
T	K	298
β	-	8.2
c_1	-	1

Table 1: Simulation parameters

4.3. Solution with adaptive quadrature

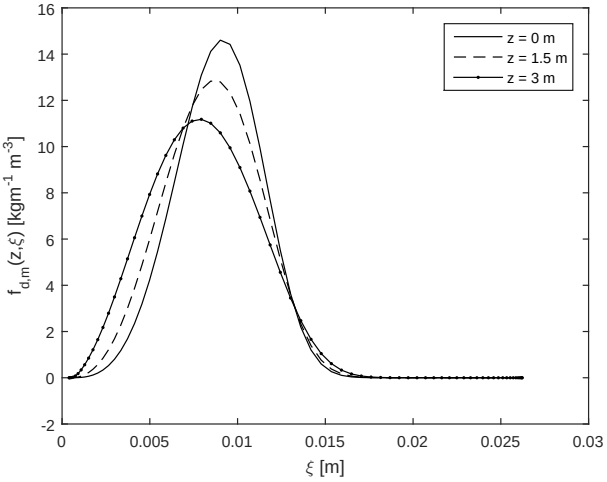

Figure 3: The solution of the PBE using the breakage kernel of Coulaloglou & Tavlarides. The distribution is shown for the inlet, middle point and outlet of the reactor.

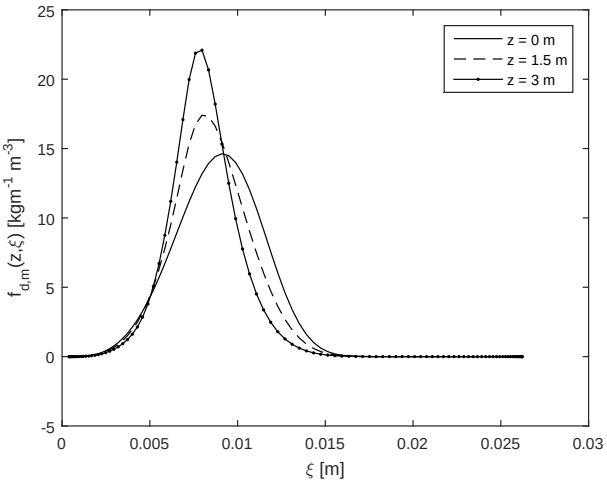

Figure 4: The solution of the PBE using the modified breakage kernel of Martinez-Bazan as given by Solsvik et al. (2017). The distribution is shown for the inlet, middle point and outlet of the reactor.

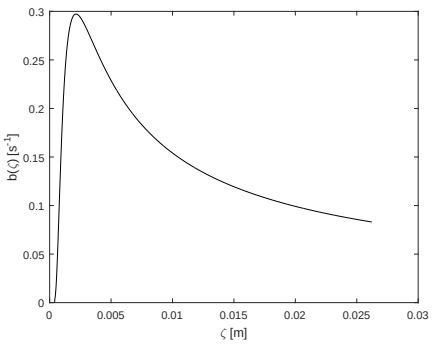

Figure 5: The calculated breakage frequency for the Coulaloglou & Tavlarides kernel as a function of mother diameter, ζ using (36). The physical data used is given in Table 1.

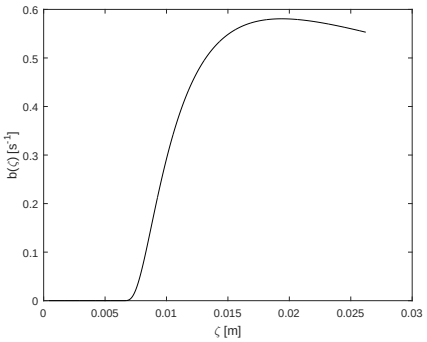

Figure 6: The calculated breakage frequency using the modified breakage kernel of Martinez-Bazan, as a function of mother diameter, ζ using (38). The physical data used is given in Table 1.

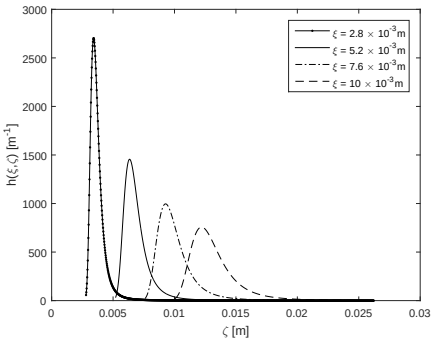

Figure 7: The calculated redistribution function for the Coulaloglou & Tavlarides kernel using (37) as a function of mother diameter, ζ. Four different daughter diameters, $\xi = 2.8 \times 10^{-3}$ m, $\xi = 5.2 \times 10^{-3}$ m, $\xi = 7.6 \times 10^{-3}$ m and $\xi = 10 \times 10^{-3}$ m are denoted by the various lines.

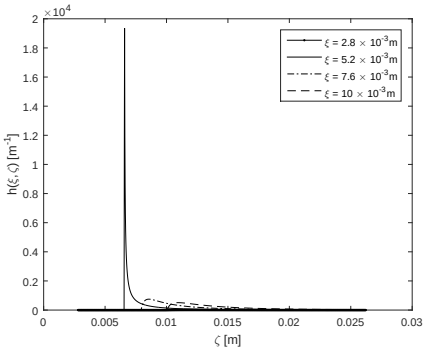

Figure 8: The calculated redistribution function using (39) as a function of mother diameter, ζ. Four different daughter diameters, $\xi = 2.8 \times 10^{-3}$ m, $\xi = 5.2 \times 10^{-3}$ m, $\xi = 7.6 \times 10^{-3}$ m and $\xi = 10 \times 10^{-3}$ m are denoted by the various lines. The modified breakage kernel of Martinez-Bazan is used.

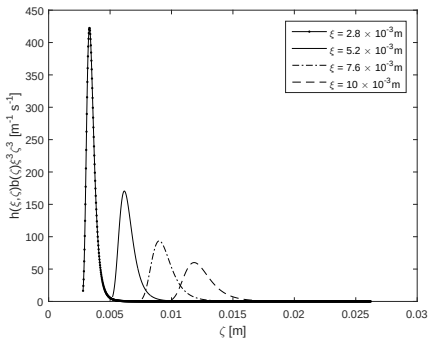

Figure 9: The calculated product of the breakage frequency (36), redistribution function (37) and the mother-daughter volume ratio, ξ^3/ζ^3, as a function of mother diameter, ζ. Four different daughter diameters, $\xi = 2.8 \times 10^{-3}$ m, $\xi = 5.2 \times 10^{-3}$ m, $\xi = 7.6 \times 10^{-3}$ m and $\xi = 10 \times 10^{-3}$ m are denoted by the various lines. The kernel of Coulaloglou & Tavlarides is used.

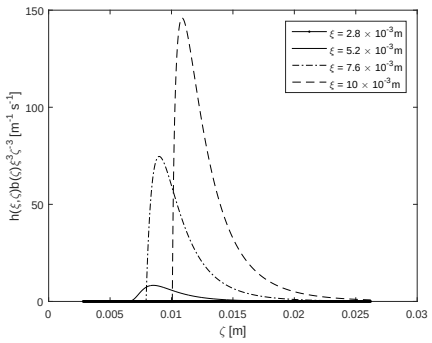

Figure 10: The calculated product of the breakage frequency (38), redistribution function (39) and the mother-daughter volume ratio, ξ^3/ζ^3, as a function of mother diameter, ζ. Four different daughter diameters, $\xi = 2.8 \times 10^{-3}$ m, $\xi = 5.2 \times 10^{-3}$ m, $\xi = 7.6 \times 10^{-3}$ m and $\xi = 10 \times 10^{-3}$ m are denoted by the various lines. The modified breakage kernel of Martinez-Bazan is used.

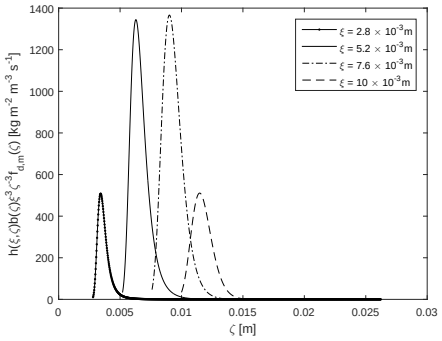

Figure 11: The calculated integral kernel using the inlet mass density distribution given in (47) in conjecture with (36) and (37) with the mother-daughter volume ratio, ξ^3/ζ^3, as a function of mother diameter, ζ. Four different daughter diameters $\xi = 2.8 \times 10^{-3}$ m, $\xi = 5.2 \times 10^{-3}$ m, $\xi = 7.6 \times 10^{-3}$ m and $\xi = 10 \times 10^{-3}$ m are denoted by the various lines. The kernel of Coulaloglou & Tavlarides is used.

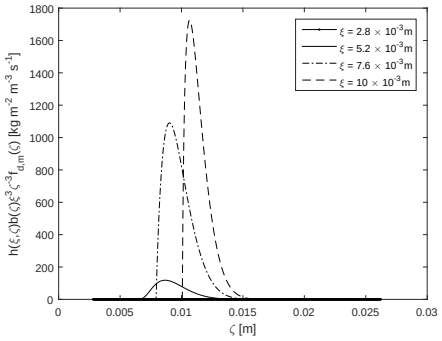

Figure 12: The calculated integral kernel using the inlet mass density distribution given in (47) in conjecture with (38) and (39) with the mother-daughter volume ratio, ξ^3/ζ^3, as a function of mother diameter, ζ. Four different daughter diameters $\xi = 2.8 \times 10^{-3}$ m, $\xi = 5.2 \times 10^{-3}$ m, $\xi = 7.6 \times 10^{-3}$ m and $\xi = 10 \times 10^{-3}$ m are denoted by the various lines. The modified breakage kernel of Martinez-Bazan is used.

The novelty of this work is in the treatment of quadrature points for the breakage birth term. Rather than working with a predefined set of quadrature points, an adaptive hp-algorithm approach taking into consideration the amount of points needed for sufficient accuracy is implemented. An alternative to a spectral fixed grid approximation for the integral term in the PBE, is to do a piece wise integration as in (27). The birth term is can then be approximated as:

$$V(\xi)\sum_{J=0}^{N_G}\sum_{e=1}^{E}\sum_{i_q=0}^{N_{q,e}} l_J^{N_G}(z_I,\zeta_{i_q,e})h(\xi_I,\zeta_{i_q,e})b(\zeta_{i_q,e})\frac{f_J}{V(\zeta_{i_q,e})}w_{i_q,e}(\zeta_{0,e},\zeta_{N_q,e}) \quad (72)$$

where the amount of quadrature elements may vary with the integration limits, $\xi \to \xi_{max}$. The objective is to find the number of elements and the quadrature order of each element that leads to a sufficient accuracy of the quadrature evaluation. A main motivation for introducing the adaptive quadrature approach used in this work is the potential loss of regularity stemming from the breakage birth kernel. The main steps in the algorithm is given as:

Step 1. Decide the lower bound of the integration.

Step 2. Use (28) and (34) to estimate interpolation error of the integral kernel for a given polynomial order.

Step 3. Use (32) and (33) if the interpolation error is too high to decide between a higher order polynomial or several integral elements.

Step 4. Repeat step 1 and 2 until the interpolation error is satisfactory.

Step 5. Compute quadrature points, quadrature weights (16) and the interpolating matrix (64).

The first step in the algorithm is to determine if the integral term with a standard set of quadrature points is sufficiently approximated. The truncated Legendre polynomial error estimator given in (34) is used for this purpose. The Legendre polynomial expansion coefficients of the breakage kernels are used.

That is, a set of Legendre basis coefficients are found through inverting the generalized Vandermonde matrix introduced in (28):

$$\begin{pmatrix} a_0 \\ a_1 \\ \vdots \\ a_N \end{pmatrix} = \begin{pmatrix} L_0(\zeta_0) & L_1(\zeta_0) & \cdots & L_N(\zeta_0) \\ L_0(\zeta_1) & L_1(\zeta_1) & \cdots & L_N(\zeta_1) \\ \vdots & \vdots & \ddots & \vdots \\ L_0(\zeta_N) & L_1(\zeta_N) & \cdots & L_N(\zeta_N) \end{pmatrix}^{-1} \begin{pmatrix} h(\xi,\zeta_0)b(\zeta_0)/V(\zeta_0) \\ h(\xi,\zeta_1)b(\zeta_1)/V(\zeta_1) \\ \vdots \\ h(\xi,\zeta_N)b(\zeta_N/V(\zeta_N)) \end{pmatrix} \tag{73}$$

If P in this case is 20, an estimate of the interpolation error of a 10th order polynomial approximation is given as:

$$\eta = \sum_{k=11}^{20} \frac{a_k^2}{k+\frac{1}{2}} \tag{74}$$

where η is the error estimator which for $P \to \infty$, $\eta = \|u - u_N\|^2_{\mathrm{L}^2(-1,1)}$. If the 10th order approximation is satisfactory, a set of quadrature points are constructed. As a Gaussian quadrature with GLL points integrate polynomials of order $2N-1$ exactly, the integrating polynomial requires a lower order than the interpolating polynomial. For the case with a 10th order interpolating polynomial, a 6th order integrating polynomial resulting in 7 quadrature points is necessary ($2 \times 6 - 1 = 11$). If the error estimator is higher than the prescribed value, a decision has to be made whether to increase the polynomial order of the expansion, or split the domain into more elements. The purpose of the hp-optimization methods is to decide which is the most efficient way to decrease the interpolation error. The hp-method used in this work is the root test algorithm of (Houston et al., 2003). An index relating to the regularity of the function is found by the use of the highest available order Legendre coefficient. Again, if $P = 20$, the root test algorithm calculates the regularity as:

$$\sigma = \frac{\log(2 \times 20 + 1) - \log(2 \times |a_{20}|^2)}{2\log 20} - \frac{1}{2} \tag{75}$$

with the kernel being regular if $\sigma > 21$. For a sufficiently regular function, an

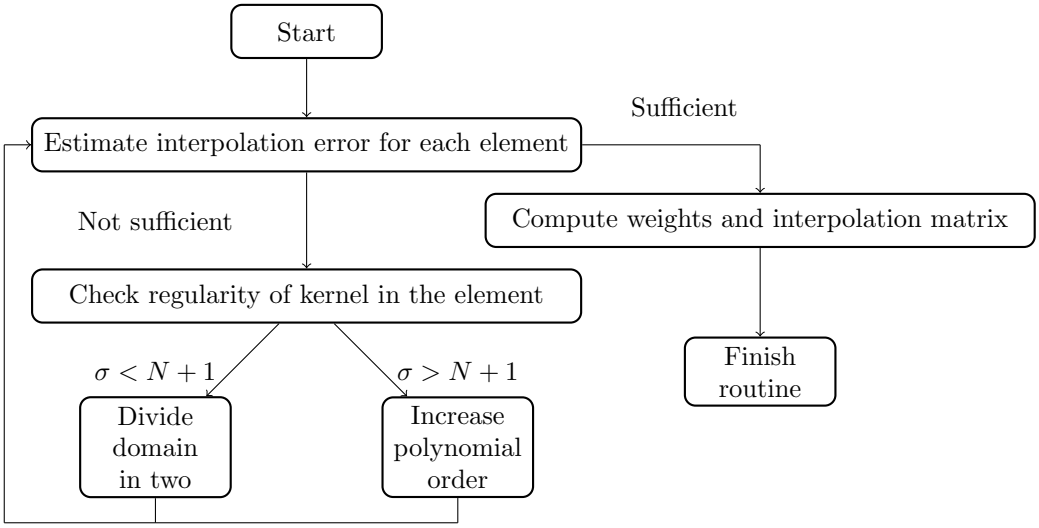

Figure 13: Flowsheet describing the computation of quadrature points. It should be noted that at the start there is only one element. This may change depending on estimated interpolation error and regularity.

increase in quadrature points should lead to an exponential decrease in integration error. If an element is under integrated according to (34), yet regular, an increase in the number of quadrature points in this element is the most beneficial.

Should however the integral be under integrated and lack this regularity, the integration domain is split into two different elements. The integration error of these two new elements is assessed and further grid refinement takes place should they be under integrated. This procedure is continued until all the elements have a calculated interpolation error less than the prescribed threshold. A flow sheet summarising this procedure is shown in Figure 13. It is emphasised that the entire integration domain is considered in the first iteration. That is, the number of elements is one.

When a set of optimal quadrature points for each element has been established, the standard spectral approach for the collocation points can be used. What is needed is a set of quadrature points consisting of the location data from the elements. These set of points, $\zeta(\xi_{i_\xi}, \xi_{max})$, can be stored as a set of vectors.

Each vector in the set consists of the quadrature points for a given integration element span. Figure 14 shows a possible set of points for the integration domain (ξ_2, ξ_7). These example sets of quadrature points consist of three elements with 3, 3 and 5 points respectively. It can however be seen from the figure that the amount of total quadrature points is only 9, given by $1 + \sum_{e=1}^{E} N_{q,e}$. This is because the common quadrature point for two elements is corresponding to the same point when integrating. Once these sets of vectors are stored, sets of interpolating matrices similar to the ones introduced previously, $\mathbf{Q}^{i_\xi}$, for interpolating from the collocation points to these quadrature points need to be constructed. In the example shown in Figure 14 the interpolation matrix takes this form:

$$\mathbf{Q}^2 = \begin{pmatrix} l_0^7(\zeta_0) & l_1^7(\zeta_0) & \cdots & l_7^7(\zeta_0) \\ l_0^7(\zeta_1) & l_1^7(\zeta_1) & \cdots & l_7^7(\zeta_1) \\ \vdots & \vdots & \ddots & \vdots \\ l_0^7(\zeta_8) & l_1^7(\zeta_8) & \cdots & l_7^7(\zeta_8) \end{pmatrix} \tag{76}$$

where it should be noted that this is not a square matrix. The matrix has 7 columns corresponding the the amount of collocation points. It has 8 rows corresponding to the quadrature points the matrix interpolates to. Lastly a set of vectors for the quadrature weights corresponding to each set of quadrature points need to be created. It is important to capture the contribution from both elements for the quadrature weight at the boundary point. This means that the quadrature weight for point ζ_2 in Figure 14 is the sum of the quadrature weights for each of the elemental domains. Once the quadrature points, interpolating matrices and quadrature weights have been constructed, the exact same procedure as outlined in the conventional spectral solution described in 4.1 can be followed. A possible procedure for this is given in Pseucocode 2.

Pseudocode 2.

1: **for** $i_\xi \leftarrow 0$ **to** N_ξ **do**

2: **compute** a set of quadrature points for a sufficient integral approximation

3: **compute** the corresponding interpolating matrix, $\mathbf{Q}^{i_\xi}$
4: **compute** the corresponding quadrature weights, $\mathbf{w}_\xi^i$
5: **end for**
6: **for** $j_z \leftarrow 0$ **to** N_z **do**
7: **for** $j_\xi \leftarrow 0$ **to** N_ξ **do**
8: **compute** $\mathrm{GM}_{j_z,j_\xi} = J$
9: **for** $i_z \leftarrow 0$ **to** N_z **do**
10: **for** $i_\xi \leftarrow 0$ **to** N_ξ **do**
11: **compute** $\mathrm{GM}_{i_z,i_\xi} = I$
12: **compute** $p(z_{i_z})$; (44)
13: **compute** $\rho_d(z_{i_z})$; (45)
14: **compute** $b(\xi_{i_\xi})$; (36) or (38)
15: $\mathbf{A}_{I,J} = v_z \mathbf{D}_{i_z,j_z} \mathbf{I}_{i_\xi,j_\xi} + \frac{\xi_{i_\xi} v_z \rho_l g}{3p(z_{i_z})} \mathbf{D}_{i_\xi,j_\xi} \mathbf{I}_{i_z,j_z} + \frac{v_z \rho_l g}{3p(z_{i_z})} \mathbf{I}_{i_z,j_z} \mathbf{I}_{i_\xi,j_\xi} -$
$b(\xi_{i_\xi}) \mathbf{I}_{i_z,j_z} \mathbf{I}_{i_\xi,j_\xi}$
16: **for** $i_q \leftarrow 0$ **to** N_q **do**
17: **compute** $b(\zeta_{i_q})$; (36) or (38)
18: **compute** $h(\zeta_{i_q}, \xi_{i_\xi})$; (37) or (39)
19: $\mathbf{A}_{I,J} = \mathbf{A}_{I,J} + \frac{\xi_{i_\xi}^3}{\zeta_{i_q}^3} \mathbf{Q}_{i_q,j_\xi}^{i_\xi} h(\zeta_{i_q} \xi_{i_\xi}) b(\zeta_{i_q}) \mathbf{w}_{i_q}^{i_\xi}$
20: **end for**
21: **end for**
22: **end for**
23: **end for**
24: **end for**

Figure 15 illustrates the calculated basis coefficients for the Legendre series expansion for the Coulaloglou & Tavlarides integral kernel shown in Figure 9. It can be seen that the coefficients have a slower decay rate for the more irregular integrands. In addition, the more irregular integrands exhibits an oscillating behavior. The case is more extreme in Figure 16 which show the basis coefficients for the the modified Martinez-Bazan kernel shown in Figure 10 for four different daughter sizes. In this case the cut off on the breakage rate leads

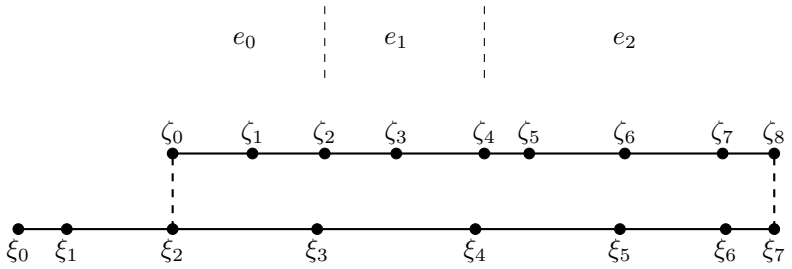

Figure 14: The relationship between the collocation points, ξ_{i_ξ}, for the mass density distribution, $f_{d,m}$, and the quadrature points corresponding to different mother bubble sizes, ζ_{i_q} in the breakage birth term. The quadrature points are in this cases divided into three elements, with $N_{q,0} = 2$, $N_{q,1} = 2$, $N_{q,2} = 4$. Each element has a GLL distribution of the quadrature points.

to severely irregular integrals. The estimated integration error using (26) for both fixed grid and adaptive quadrature are given in Figure 17 for Coulaloglou & Tavlarides and Figure 18 for Martinez-Bazan. A daughter size of 2.8×10^{-3}m has been used. A very high order fixed grid quadrature approximation is used as an estimate of the exact solution.

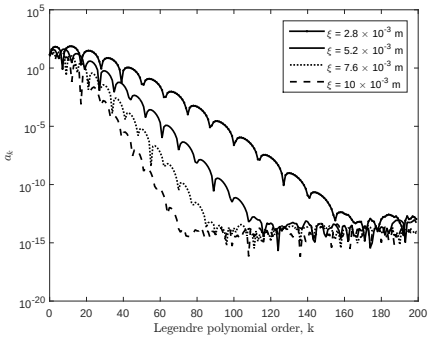

Figure 15: The calculated absolute value of the Legendre expansion coefficients using (19) for the integral kernel of Coulaloglou & Tavlarides. Four different daughter diameters $\xi = 2.8 \times 10^{-3}$ m, $\xi = 5.2 \times 10^{-3}$ m, $\xi = 7.6 \times 10^{-3}$ m and $\xi = 10 \times 10^{-3}$ m are shown with the various lines.

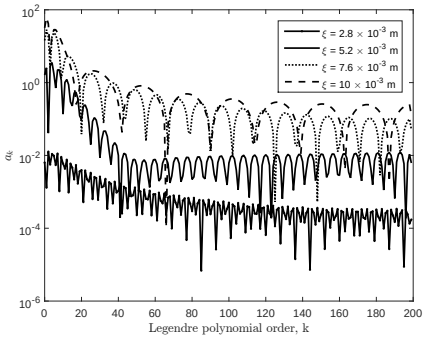

Figure 16: The calculated absolute value of the Legendre expansion coefficients using (19) for the modified integral kernel of Martinez-Bazan. Four different daughter diameters $\xi = 2.8 \times 10^{-3}$ m, $\xi = 5.2 \times 10^{-3}$ m, $\xi = 7.6 \times 10^{-3}$ m and $\xi = 10 \times 10^{-3}$ m are shown with the various lines.

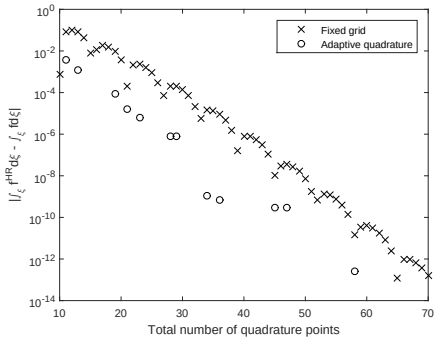

Figure 17: The estimated absolute value of the difference between the exact and approximated evaluation of the breakage birth integral for the Coulaloglou & Tavlarides kernel. The daughter diameter is taken to be $\xi = 2.8 \times 10^{-3}$m.

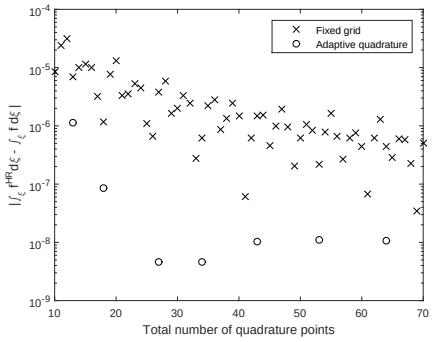

Figure 18: The estimated absolute value of the difference between the exact and approximated evaluation of the breakage birth integral for the modified Martinez-Bazan kernel. The daughter diameter is taken to be $\xi = 2.8 \times 10^{-3}$m.

5. Result and Discussion

Two different breakage closures have been used in order to validate the adaptive quadrature method. The PBE using both closures were solved for a residual close to machine accuracy in MATLAB using the orthogonal collocation method, with a fixed and adaptive set of quadrature points.

Figures 17 and 18 show the accuracy of integration of the breakage kernel using the standard GLL quadrature point solution, and the adaptive approach. The x-axis describe the total amount of quadrature points used. The y-axis is in a log scale and is calculated using the definition on the left hand side of (26). The exact solution of the integral is taken to be a very high resolution standard quadrature approximation of the integral. The circles representing the adaptive approach are calculating using different error tolerances for the adaptive approach. This is an adjustable parameter in the method. It can be seen that the breakage kernel is evaluated more accurately, with fewer quadrature points using the adaptive approach for both breakage kernels. The convergence rate of the adaptive quadrature approach seem to taper off at around a difference of about 10×10^{-9}. This is likely due to the fact that many of the coefficients, a_k, are around machine accuracy, making it more difficult to assess the regularity due to roundoff errors. This might make the method less robust at these tolerances. The total number of quadrature points needed still remains below that of the standard approach for all error tolerances. In the case of the modified Martinez-Bazan closure the decrease in error when compared to the fixed approach decreases more rapidly than for the Coulaloglou & Tavlarides kernel. This is not unexpected in view of the calculated expansion coefficients for the two kernels shown in Figures 15 and 16. The modified Martinez-Bazan closure contains very steep gradients.

Figures 19 and 23 shows the calculated difference in mass of bubbles flowing in and out of the reactor for the kernels of Coulaloglou & Tavlarides and the modified Martinez-Bazan, respectively, as a function of the number of colloca-

tion points used in the ξ-coordinate. The standard solver consists of a fixed grid of quadrature points set equal to the number of collocation points, while the adaptive quadrature solver adapts to an optimal number of quadrature points. The criterion for mass conservation is based on (71). In order to plot the results on a logarithmic scale, the following normalized criterion was plotted on the y-axis in Figures 19 and 23:

$$\epsilon = \left| 1 - \frac{\int_{\Omega_\xi} f_{d,m}(z_{end}, \xi) \mathrm{d}\xi}{\int_{\Omega_\xi} f_{d,m}(z_0, \xi) \mathrm{d}\xi} \right| \tag{77}$$

where the quadrature points for this integration coincide with the collocation points for the mass density function. Figure 19 shows that there is a better mass conservation through the reactor when using the adaptive quadrature approach as opposed to the fixrd grid approach for the Coulaloglou & Tavlarides kernel. The change in mass conservation with respect to the amount of collocation points is also more stable than the standard approach. This is likely due to oscillating behavior of the Legendre basis coefficient of the integral kernel as shown in Figure 15, whereas the adaptive approach has a defined criterion for the quadrature point placement. However Figure 23 show that this difference in mass in and out of the reactor is only marginal in the case of the modified Martinez-Bazan kernel. The reason for this is that the numerical resolution of the mass density function is the major limitation for this solution. Related to this, the convergence rate towards a grid independent solution is the same for both the adaptive and fixed case using the modified Martinez-Bazan kernel as seen in Figure 26. Whilst for the Coulaloglou & Tavlarides kernel the adaptive quadrature approach needs fewer collocation points to reach grid independence, seen in Figure 22. The lack of complete mass conservation in the systems at grid independent numerical resolution is likely due to the fact that the daughter redistribution kernels used is not completely volume, and by extension, mass conserving (Solsvik et al., 2013).

A second criterion is related to the birth and death operators in the system

of equations and the calculated mass density distribution, (70):

$$\int_{\Omega} (\mathbf{A}^{\text{Birth}} - \mathbf{A}^{\text{Death}}) \mathbf{f} \mathrm{d}\Omega = 0 \tag{78}$$

The calculated difference in between the birth and death operators as a function of the number of collocation points are shown in Figure 20 for Coulaloglou & Tavlarides and Figure 24 for the modified Martinez-Bazan. In both cases the adaptive quadrature approach seem to show an improvement over the fixed approach. Again this is categorically true for Coulaloglou & Tavlarides case, whilst for the modified Martinez-Bazan it is a more modest improvement.

The results show that both the number of quadrature points and collocation points have an impact on the accuracy of the solution. In the adaptive quadrature approach however, there is always a sufficient amount of quadrature points meaning that it is the true effect of the amount of collocation points which is found. The condition number for the system matrix for both cases are shown in Figures 21 and 25 for Coulaloglou & Tavlarides and Martinez-Bazan respectively. The condition number in the L^2 norm is calculated as:

$$\kappa = \|\mathbf{A}\| \|\mathbf{A}^{-1}\| \tag{79}$$

which for Coulaloglou & Tavlarides seem to favor the adaptive quadrature approach, whilst it is identical for the modified Martinez-Bazan kernel. Although all calculated condition numbers are so low that this is very unlikely to make a noticeable difference when solving the system.

Figures 22 and 26 show an estimated L^2 error. For a lack of a better estimate, a high resolution standard approach is used as benchmark. It can been that in for Coulaloglou & Tavlarides, the adaptive approach leads to needing a fewer number of collocation points for a grid independent solution. The same trend as for the error in mass conservation is present for the modified Martinez-Bazan. Dorao and Jakobsen (2008) did use the hp-approach for solving the density function, an approach that might be beneficial for the modified Martinez-Bazan case.

One drawback of the adaptive quadrature approach is that there is an increase in the computational overhead required to construct the system matrix. For a stand alone solution of the PBE this extra computational cost might make an adaptive approach undesirable. If however the PBE should be solved multiple times, for instance in a multi-fluid model or dynamic models, the increased computational performance might be considerable. In this implementation a single quadrature point optimization will lead to an efficient set quadrature points, allowing the number of collocation points to be reduced which in turn reduces the size of the system matrix. For the Coulaloglou & Tavlarides kernel, 20 collocation points in the property space is a sufficient number. For the standard approach the necessary number of collocation points is 30. In addition there is a decrease in the amount of quadrature points needed. For the case of the modified Martinez-Bazan kernel, the better mass conservation for the adaptive quadrature approach seem to only appear at a higher number of collocation points.

In order to further investigate how the increased overhead costs and reduced system size might affect computational performance, the running times to achieve roughly the same error in mass conservation for the two kernels, using both the standard approach and the adaptive approach, were computed. The test was performed using MATLAB2015a, on a Windows 10.0.16299 system with an Intel Xeon-E5-2697v4 CPU. The system had a total memory of 32 GB, 2400 MHz. The codes were not optimized to decrease running times, but should nevertheless be comparable. The running times were taken to be the average of 100 runs. The simulation times are presented in Table 2. Two sets of computational times are given. The first set is the total time required to calculate all the points, quadrature weights, interpolation matrices and the adaptive mesh, in addition to solving the system of equations. The second set, under the heading A & T (Assembly and Inversion), is the average time to assemble and solve the system of equations given pre calculated points, quadrature weights and interpolation matrices. Also given are the number of collocation

Breakage kernel and method	Error in mass cons.	Total time	A & I time	N_ξ	$\sum N_q$
C & T, standard approach	6.3×10^{-5}	0.61 s	1.52×10^{-2} s	30	900
C & T, adaptive quadrature	5.9×10^{-5}	1.2 s	4.52×10^{-3} s	20	363
MB, standard approach	3.4×10^{-4}	7.1 s	1.43×10^{-1} s	50	2500
MB, adaptive quadrature	4.2×10^{-5}	5.6 s	5.54×10^{-2} s	35	834

Table 2: Simulation time from scratch to a solved system.

points used, the error in mass conservation of the solution and the total number of interpolation points used to integrate the source term, $\sum N_q$. In order to evaluate the integral, the interpolation to each quadrature point is necessary. As expected, the adaptive quadrature approach leads to the least amount of interpolation needed to accurately estimate the integral.

The assembly and inversion time using the adaptive grid is roughly one third of the time used with the standard grid for both breakage kernels. Using the same sets of points and weights for an iterative system, the main computational cost would be to find the coefficients for the system matrix and to invert it. The use of fewer interpolation points will lead to faster computation of these coefficients, while the use of fewer collocation points will lead to both quicker computation of coefficients and a faster inversion of the system matrix. This means that the adaptive quadrature approach has the potential to increase the computational speed of the numerically demanding weighted residual methods, in particular, for iterative and coupled systems. The adaptive quadrature method could be very useful for systems where the optimum grid points do not change appreciably between iterations, allowing sporadic updates on the optimum grid. Examples of these types of systems are CFD simulations, where the system does not change significantly in time or space.

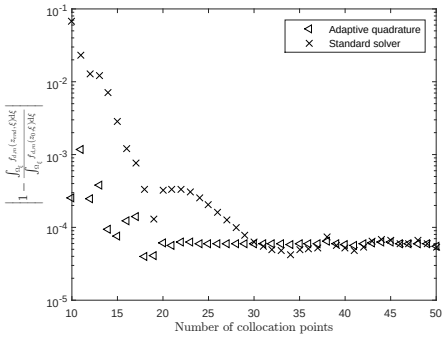

Figure 19: The difference in the mass of the dispersed phase flowing in and out of the reactor for the Coulaloglou & Tavlarides kernel. The mass difference is calculated as $\epsilon = |1 - \frac{\int_{\Omega_\xi} f_{d,m}(z_{end},\xi)\mathrm{d}\xi}{\int_{\Omega_\xi} f_{d,m}(z_0,\xi)\mathrm{d}\xi}|$.

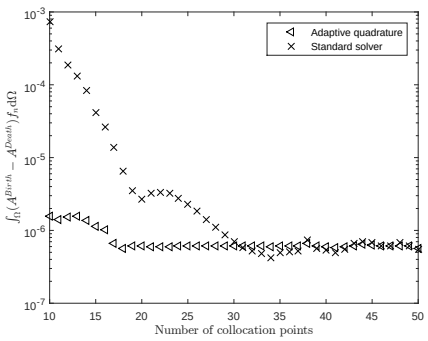

Figure 20: The difference between the breakage birth and death problem operator matrices through the reactor for the Coulaloglou & Tavlarides kernel.

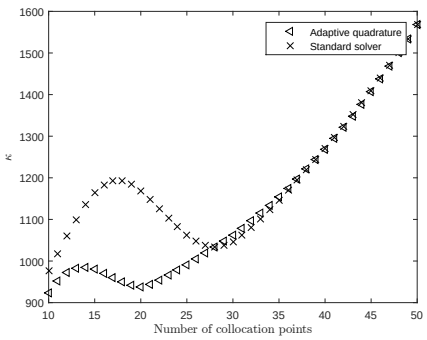

Figure 21: The calculated condition number for the problem operator matrix for the Coulaloglou & Tavlarides kernel using (79).

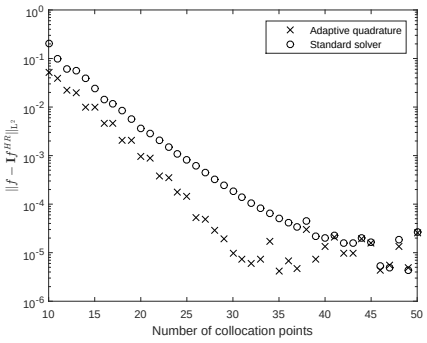

Figure 22: The L^2-norm of the solution with the Coulaloglou & Tavlarides kernel for both the standard and adaptive approach. The high resolution solution is taken to be the reference.

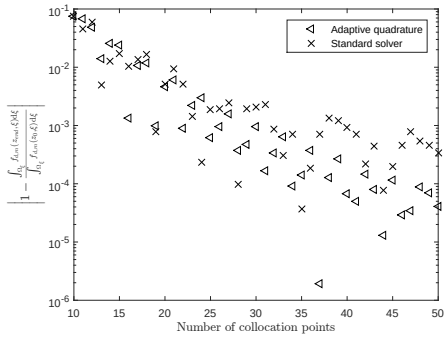

Figure 23: The difference in the mass of the dispersed phase flowing in and out of the reactor for the modified Martinez-Bazan kernel. The mass difference is calculated as $\epsilon = |1 - \frac{\int_{\Omega_\xi} f_{d,m}(z_{end},\xi)\mathrm{d}\xi}{\int_{\Omega_\xi} f_{d,m}(z_0,\xi)\mathrm{d}\xi}|$.

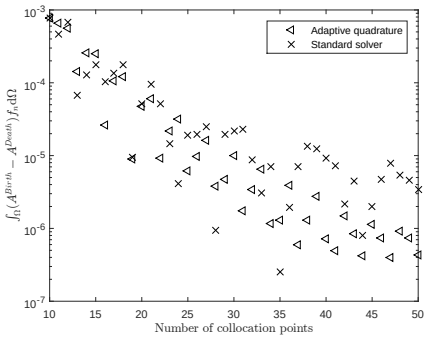

Figure 24: The difference between the breakage birth and death problem operator matrices through the reactor for the modified Martinez-Bazan kernel.

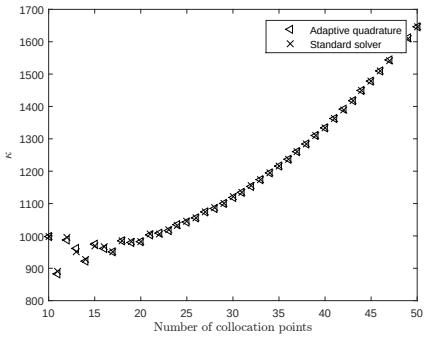

Figure 25: The calculated condition number for the problem operator matrix for the modified Martinez-Bazan kernel using (79).

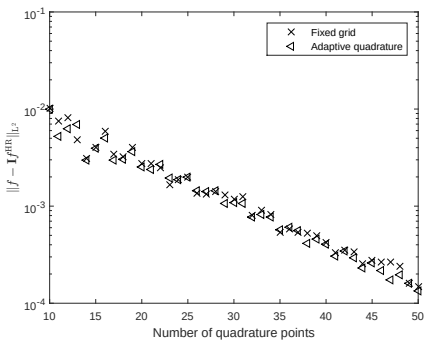

Figure 26: The L^2-norm of the solution of the modified Martinez-Bazan kernel for both the standard and adaptive approach. The high resolution solution is taken to be the reference.

6. Conclusion

An adaptive quadrature approach to solve the PBE has been implemented based on a hp-optimization approach. The method has been tested with two different breakage kernels. The adaptive quadrature procedure gave equal or better results with respect to number of collocation points needed for a grid independent solution, than previously implemented fixed grid approaches to solving the PBE using a weighted residuals method. The criterion used is the error in mass conservation of the mass density distribution function which is solved for, both in the system matrix and for the inlet and outlet mass of bubbles in the reactor. The implemented method is especially suitable for iterative and breakage dominated systems. These types of systems might for example be in intensely turbulent regions with a high turbulent dissipation rate. The total integration time for variable coefficient systems is roughly halved in the investigated cases, potentially saving significant computational time. For systems where the breakage birth integral term is not dominated by the daughter redistribution function, the adaptive quadrature approach presented in this work might not be as beneficial. The method might still be useful, as it ensures that the accuracy of the integral approximation is not the limiting factor of the numerical method.

When solving several coupled reactor model equations, the more efficient set of grid points may lead to a significant decrease in computational time. For both the example cases used, the system matrix of the adaptive quadrature approach is half the size of the fixed grid system matrix. For every inversion of the PBE system matrix, the computational time is reduced by around 65 %. The potential gains per iteration of the PBE solution seem to be larger than the increase in overhead for the adaptive procedure.

Recommendations for future work include comparing the adaptive quadrature approach with the standard method for a more complex reactor model. Future work may investigate whether the adaptive quadrature approach is fea-

sible for the PBE coalescence terms and dynamic systems.

Acknowledgements

This work was supported by the program "NTNU Biotechnology - the confluence of Life Sciences, Mathematical Sciences and Engineering" (M. Engh).

Declarations of interest: none.

Author contributions

M. Engh implemented the adaptive quadrature algorithm and wrote the manuscript. J Solsvik provided parts of the code for the standard solver. H.A. Jakobsen contributed with many suggestions and corrected the manuscript.

References

Attaraikh, M. M., Drumm, C., Bart, H.-J., 2009. Solution of the population balance equation using the sectional quadrature method of moments (sqmom). Chemical Engineering Science 64, 742–752.
DOI: 10.1016/j.ces.2008.05.006

Attarakih, M., Bart, H.-J., 2018. Solution of the population balance equation: From global to local constrained maximum entropy method. In: Gernaey, K. V., Briesen, H., Kumar, J., Nopens, I. (Eds.), 6th International Conference on Population Balance Modelling: Conference Proceedings. May 6-9, Ghent, Belgium.

Canuto, C., Hussaini, M. Y., Quarteroni, A., Zang, T. A., 2006. Spectral Methods: Fundamentals in Single Domains. Scientific Computation. Springer Berlin Heidelberg, Berlin, Heidelberg.
DOI: 10.1007/978-3-540-30726-6

Coulaloglou, C. A., Tavlarides, L. L., 1977. Description of interaction processes in agitated liquid-liquid dispersions. Chemical Engineering Science 32 (11), 1289–1297.
DOI: 10.1016/0009-2509(77)85023-9

Dorao, C. A., september 2006. High order methods for the solution of the population balance equation with applications to bubbly flows. Ph.D. thesis.

Dorao, C. A., Jakobsen, H. A., 2008. Hp-Adaptive Least Squares Spectral Element Method for Population Balance Equations. Applied Numerical Mathematics 58 (5), 563–576.
DOI: 10.1016/j.apnum.2006.12.005

Finlayson, B., Scriven, L., 1966. The Method of Weighted Residuals - A review. Applied Mechanics Review 19 (9), 735–748.

Golub, G. H., Welsch, J. H., 1969. Calculation of Gauss Quadrature Rules. Mathematics of Computation 23 (106), 221.
DOI: 10.2307/2004418

Hale, N., Townsend, A., jan 2013. Fast and Accurate Computation of Gauss–Legendre and Gauss–Jacobi Quadrature Nodes and Weights. SIAM Journal on Scientific Computing 35 (2), A652–A674.
DOI: 10.1137/120889873

Houston, P., Senior, B., Suli, E., 2003. Sobolev Regularity Estimation for hp-Adaptive Finite Element Methods. Numerical Mathematics and Advanced Applications, 619–644.
DOI: 10.1007/978-88-470-2089-4_58

Houston, P., Süli, E., 2005. A note on the design of hp-adaptive finite element methods for elliptic partial differential equations. Computer Methods in Applied Mechanics and Engineering 194 (2-5 SPEC. ISS.), 229–243.
DOI: 10.1016/j.cma.2004.04.009

809 Jakobsen, H. A., 2014. Chemical Reactor Modeling, Multiphase Reactive Flows,
810 2nd Edition. Springer-Verlag.
811 DOI: 10.1007/978-3-319-05092-8

812 Karniadakis, G., Sherwin, S., 2005. Spectral/hp Element Methods for Compu-
813 tational Fluid Dynamics, 2nd Edition. Oxford university press.
814 DOI: 10.1093/acprof:oso/9780198528692.001.0001

815 Kumar, S., Ramkrishna, D., 1996. On the Solution of the Population Balance
816 Equations bu Discretizations - I. A fixed pivot technique. Chemical Engineer-
817 ing Science 51 (8), 1311–1332.

818 Marchisio, D. L., Fox, R. O., 2005. Solution of population balance equations
819 using the direct quadrature method of moments. Aerososol Science 36, 43–73.

820 Marchisio, D. L., Fox, R. O., 2013. Computational Models for Polydisperse
821 Particulate and Multiphase Systems. Cambridge university press, Cambridge.

822 Martinez-Bazan, C., Rodriguez-Rodriguez, J., Deane, G., Montanes, J.,
823 Lasheras, J., 2010. Considerations on bubble fragmentation models . Jour-
824 nal of Fluid Mechanics 661, 159–177.
825 DOI: 10.1017/S0022112010003186

826 Mcgraw, R., 1997. Description of Aerosol Dynamics by the Quadrature Method
827 of Moments Quadrature Method of Moments. Aerosol Science and Technology
828 6826.
829 DOI: 10.1080/02786829708965471

830 Mead, L. R., Papanicolaou, N., 1984. Maximum entropy in the problem of
831 moments. Journal of Mathematical Physics 2404 (25).

832 Nayak, A. K., Borka, Z., Patruno, L. E., Sporleder, F., Dorao, C. A., Jakobsen,
833 H. A., 2011. A Combined Multifluid-Population Balance Model for Vertical
834 Gas - Liquid Bubble-Driven Flows Considering Bubble Column Operating
835 Conditions. Industrial & Engineering Chemistry Research 50, 1786–1798.
836 DOI: 10.1021/ie101664w

Nguyen, T. T., Laurent, F., Fox, R. O., Massot, M., 2016. Solution of population balance equations in applications with fine particles : Mathematical modeling and numerical schemes. Journal of Computational Physics 325, 129–156.
DOI: 10.1016/j.jcp.2016.08.017

Pigou, M., Morchain, J., Fede, P., Penet, M.-I., Laronze, G., 2018. A new moment-inversion procedure for the extended quadrature method of moments. In: Gernaey, K. V., Briesen, H., Kumar, J., Nopens, I. (Eds.), 6th International Conference on Population Balance Modelling. May 6-9, Ghent, Belgium.

Prince, M. J., Blanch, H. W., 1990. Bubble Coalescence and Breakup in Air Sparged Bubble Columns. AIChE Journal 36 (10), 1485–1499.
DOI: https://doi.org/10.1002/aic.690361004

Quarteroni, A., 2014. Numerical Models for Differential Problems, 2nd Edition. Springer Milan, Milano.
DOI: 10.1007/978-88-470-5522-3

Ramkrishna, D., 2000. Population Balances. Theory and Applications to Particulate Systems in Engineering, 1st Edition. Academic Press, San Diego.

Solsvik, J., Becker, P. J., Sheibat-othman, N., Jakobsen, H. A., 2016. Numerical Solution of the Drop Population Balance Equation Using Weighted Residual and Finite Volume Methods. Journal of Dispersion Science and Technology, 80–88.
DOI: 10.1080/01932691.2015.1028550

Solsvik, J., Jakobsen, H. A., 2013a. Evaluation of weighted residual methods for the solution of a population balance model describing bubbly flows: The least-squares, Galerkin, tau, and orthogonal collocation methods. Industrial and Engineering Chemistry Research 52 (45), 15988–16013.
DOI: 10.1021/ie402033b

Solsvik, J., Jakobsen, H. A., 2013b. On the solution of the population balance equation for bubbly flows using the high-order least squares method: implementation issues. Reviews in Chemical Engineering 29 (2), 63–98.
DOI: 10.1515/revce-2012-0018

Solsvik, J., Skjervold, V. T., Jakobsen, H. A., 2017. A bubble breakage model for finite Reynolds number flows. Journal of Dispersion Science and Technology 38 (7), 973–978.
DOI: 10.1080/01932691.2016.1216440

Solsvik, J., Tangen, S., Jakobsen, H. A., 2013. On the constitutive equations for fluid particle breakage. Reviews in Chemical Engineering 29 (5), 241–356.
DOI: 10.1515/revce-2013-0009

Vik, C. B., Solsvik, J., Hillestad, M., Jakobsen, H. A., 2018. A multifluid-PBE model for simulation of mass transfer limited processes operated in bubble columns. Computers and Chemical Engineering 110, 115–139.
DOI: 10.1016/j.compchemeng.2017.11.023

Wulkow, M., Gerstlauer, A., Nieken, U., 2001. Modeling and simulation of crystallization processes using parsival. Chemical Engineering Science 56, 2575–2588.

Yaghini, N., Iedema, P. D., 2014. Molecular weight / branching distribution modeling of low-density-polyethylene accounting for topological scission and combination termination in continuous stirred tank reactor. Chemical Engineering Science 116, 144–160.
DOI: 10.1016/j.ces.2014.04.039

Yuan, C., Fox, R. O., Sep. 2011. Conditional quadrature method of moments for kinetic equations. J. Comput. Phys. 230 (22), 8216–8246.
DOI: 10.1016/j.jcp.2011.07.020

Yuan, C., Laurent, F., Fox, R. O., 2012. An extended quadrature method of moments for population balance equations. Journal of Aerosol Science 51, 1–

23.
DOI: 10.1016/j.jaerosci.2012.04.003

Zhu, Z., Dorao, C. A., Jakobsen, H. A., 2008. A least-squares method with direct minimization for the solution of the breakage-coalescence population balance equation. Mathematics and Computers in Simulation 79 (3), 716–727.
DOI: 10.1016/j.matcom.2008.05.001